

## Research article

# Multicomponent comprehensive confirms that erythroferrone is a molecular biomarker of pan-cancer

Ying Cai<sup>a,b,1</sup>, Yaling Gao<sup>c,1</sup>, Yinyin Lv<sup>a,b</sup>, Zhiyuan Chen<sup>a,b</sup>, Lingfeng Zhong<sup>a,b</sup>, Junjie Chen<sup>a,b</sup>, Yanyun Fan<sup>a,b,\*</sup>

<sup>a</sup> Department of Gastroenterology, Zhongshan Hospital of Xiamen University, School of Medicine, Xiamen University, Xiamen, Fujian, PR China

<sup>b</sup> Xiamen Key Laboratory of intestinal microbiome and human health, Zhongshan Hospital affiliated to Xiamen University, Xiamen, Fujian, PR China

<sup>c</sup> Department of Xia He, Zhongshan Hospital of Xiamen University, School of Medicine, Xiamen University, Xiamen, Fujian, PR China

## ARTICLE INFO

## Keywords:

ERFE  
Pan-cancer analysis  
Prognostic biomarker  
Molecular biomarker  
Omics integrative analysis

## ABSTRACT

All vertebrates organisms produce erythroferrone, a secretory hormone with structure-related functions during iron homeostasis. However, limited knowledge exists regarding the effect of this hormone on the occurrence and progression of cancer. To systematically and comprehensively identify the diverse implications of Erythroferrone (ERFE) in various malignant tumors, we conducted an in-depth analysis of multiple datasets, including the expression levels of oncogenes and target proteins, biological functions, and molecular characteristics. This analysis aimed to assess the diagnostic and prognostic value of ERFE in pan-cancer. Our findings revealed a significant elevation in ERFE expression across 20 distinct cancer types, with notable increases in gastrointestinal cancers. Utilizing the Cytoscape and STRING databases, we identified 35 ERFE-targeted binding proteins. Survival prognosis studies, particularly gastrointestinal cancers indicated by Colon adenocarcinoma (COAD), demonstrated a poor prognosis in patients with high ERFE expression ( $p < 0.001$ ), consistently observed across various clinical subgroups. Furthermore, the ROC curve underscored the high predictive ability of ERFE for gastrointestinal cancer ( $AUC > 0.9$ ). Understanding the roles and interactions of ERFE in biological processes can also be aided by examining the genes co-expressed with ERFE in the COAD and ranking the top 50 positive and negative genes. In the correlation analysis between the ERFE gene and different immune cells in COAD, we discovered that the expression of ERFE was positively correlated with Th1 cells, cytotoxic cells, and activated DC (aDC) abundance, and negatively correlated with Tcm (T central memory) abundance ( $P < 0.001$ ). In summary, ERFE emerges as strongly associated with various malignant cancers, positioning it as a prospective biological target for cancer treatment. It stands out as a key molecular biomarker for diagnosing and prognosticating pancreatic cancer, also serves as an independent prognostic risk factor for COAD.

\* Corresponding author. Department of Gastroenterology, Zhongshan Hospital of Xiamen University, School of Medicine, Xiamen University, Xiamen, Fujian, PR China.

E-mail addresses: [18883939814@163.com](mailto:18883939814@163.com) (Y. Cai), [gao\\_yaling@126.com](mailto:gao_yaling@126.com) (Y. Gao), [lvyi2016\\_xmu@163.com](mailto:lvyi2016_xmu@163.com) (Y. Lv), [chenzy\\_98@163.com](mailto:chenzy_98@163.com) (Z. Chen), [179303298@qq.com](mailto:179303298@qq.com) (L. Zhong), [1227732383@qq.com](mailto:1227732383@qq.com) (J. Chen), [fanyanyun@xmu.edu.cn](mailto:fanyanyun@xmu.edu.cn) (Y. Fan).

<sup>1</sup> Represents the same contribution to this article.

<https://doi.org/10.1016/j.heliyon.2024.e26990>

Received 4 August 2023; Received in revised form 1 February 2024; Accepted 22 February 2024

Available online 26 February 2024

2405-8440/© 2024 The Authors. Published by Elsevier Ltd. This is an open access article under the CC BY-NC-ND license (<http://creativecommons.org/licenses/by-nc-nd/4.0/>).

## 1. Introduction

Iron is a crucial micronutrient for almost all species owing to its critical functions in catalytic redox reactions, oxygen transport, and storage. Ferritin, the sole homeostatic hormone responsible for controlling plasma iron levels and total body iron content, regulates the flow of iron into the body [1,2]. When the oxygen supply to the tissue cannot meet the demand, interstitial fibroblasts detect hypoxia and begin producing and releasing erythropoietin (EPO). The production of EPO is regulated by hypoxia-inducible factor 2 (HIF-2) transcription. However, in vitro studies have indicated that EPO does not inhibit the release of ferritin from hepatocytes [3], implying the existence of an intermediary EPO reactive ferritin inhibitor. The transcript Fam132b, which has been renamed Erfe, is induced and maintains high expression for 24–48 h just before ferritin inhibition, consistent with the evidence that erythropoietic activity affects ferritin expression [4–7]. While erythroferrone protein has been previously categorized as C1q/tumor necrosis factor (TNF)-related protein 15 (CTRP15) and myonectin [8], its novel primary function in controlling ferritin and iron homeostasis is noteworthy. In addition to elucidating the reported iron regulatory responses to conditions such as anemia, bleeding, hypoxia, and disorders of inefficient erythropoiesis such as thalassemia and myelodysplastic syndrome, ERFE fulfills the criteria for identifying potential erythrocyte regulators of iron homeostasis.

All vertebrates contain creatures include erythroferrone, a member of the CTRP family of secretory hormones associated with structure [9]. The four-domain ERFE shares high sequence homology with other family members at the C-terminus, similar to other CTRP, and has a distinct N-terminus [10,11]. All vertebrate genomes contain the ERFE gene, demonstrating its importance in the physiology of several life forms. The stability of iron transporters facilitates the mobilization of cellular stored iron to the plasma, making it available for utilization by mature erythrocytes, accompanied by the stimulation of erythropoiesis. It is now acknowledged as the primary erythrocyte regulator of iron homeostasis [12,13]. Vertebrates can respond to blood loss and recover swiftly from it thanks to this crucial regulatory axis.

Colorectal cancer (CRC) is among the most prevalent malignancies of the digestive system worldwide. Rectal cancer is the eighth most common malignant tumor worldwide, whereas colon cancer is the fourth most common. CRC accounts for 11% of all cancer cases diagnosed worldwide and is the third most common type cancer [14]. CRC is also the second-deadliest cancer worldwide [15]. CRC is one of the top five confirmed causes of cancer and cancer-related deaths in China is CRC [16]. The prevalence of CRC decreases with extensive colonoscopy. Colectomy, chemotherapy, and immunotherapy are only a few of the newer treatments available for patients with colon cancer patients, and their overall 5-year relative survival rate is approximately 64% [17]. Although colon cancer is linked to nutrition, microbes, and their metabolites, the precise mechanisms of its development remain unknown [18]. Therefore, it is crucial to understand the molecular basis of colon cancer.

We are unsure of ERFE's function in cancer; therefore, we questioned whether it can influence the onset and progression of various cancer types. To the best of our knowledge, in order to provide a more systematic and thorough understanding of ERFE, we first discussed its expression and biological function from a pan-cancer perspective, concentrating on its diagnostic and prognostic value. We discovered that ERFE was significantly up-regulated not only in 20 different types of human cancers, but also in digestive tract tumors. Moreover, there was a strong correlation between the degree of ERFE expression and the Overall Survival (OS), Disease Specific Survival (DSS) and Progression Free Interval (PFI) of gastrointestinal cancers, particularly Liver hepatocellular carcinoma (LIHC), Colon adenocarcinoma (COAD), Stomach adenocarcinoma (STAD) and Colon adenocarcinoma/Rectum adenocarcinoma Esophageal carcinoma (COADREAD). We narrowed our attention to COAD and identified ERFE as a distinct risk factor for OS, DSS, and PFI in COAD. Additionally, we examined the co-expression of genes that were favorably and negatively correlated with ERFE, as well as how these genes are related to other immune cells. ERFE is a viable molecular target for COAD and, taken collectively, may be a potential biomarker for pan-cancer diagnosis and prognosis.

## 2. Materials and methods

### 2.1. Gene expression analysis

UCSC XENA (<https://xenabrowser.net/datapages/>) obtained the RNA-seq data and relevant clinical information for 15,776 samples, encompassing 33 tumor types and normal tissues sourced from the Genotype-Tissue Expression (GTEx) and Cancer Genome Atlas (TCGA) databases. It helps us discover the differential genes between tumor types and normal tissues to explore their feasibility and practicality. The Cancer Cell Line Encyclopedia (CCLE) database (<https://portals.broadinstitute.org/ccle/>) was used to download the information about tumor cell lines. The ggplot2 package was used for visualization, and R software 3.6.3 was utilized for statistical analysis. Two sets of data were identified through the Wilcoxon rank sum test, and  $p \leq 0.05$  was deemed statistically significant (ns,  $p \geq 0.05$ ; \*,  $p < 0.05$ ; \*\*,  $p < 0.01$ ; \*\*\*,  $p < 0.001$ ).

### 2.2. Cell culture and RT-qPCR assay

HCoEPIC (Item No. CP-H122) was purchased from Tongpai Biotechnology Co., Ltd. (Shanghai, China). SW480, SW620, HCT116, HCT15, HT29, and CT26 were purchased from the Cell Bank of the Chinese Academy of Sciences. Cells were added with the corresponding medium according to the instructions and placed in a cell culture incubator at 37 °C with 5% CO<sub>2</sub>. After RNA extraction from the cells, RNA reverse transcription was performed using the PrimeScript™ RT kit from Takara, Japan, and ERFE mRNA expression was detected by SYBR® premix ExTaq™ II (Takara). RT-qPCR was performed using a fluorescence quantitative PCR instrument-9 LightCycler 480II (ROCHE). RT-qPCR primers for ERFE and  $\beta$ -actin were as follows: ERFE forward, 5'-ATG-GGG-CTG-GAG-AAC-

AGC-3', reverse, 5'-TGG-CAT-TGT-CCA-AGA-AGA-CA-3'; and  $\beta$ -actin forward, 5'-AGGCTCTTTCCAGCCTTCC -3', reverse, 5'-CTGTCAGCAATGCCAGGGGTA-3'.

### 2.3. Protein-protein interaction network Building

By configuring the following key parameters: minimum needed interaction score ["medium confidence (0.400)"] and active interaction sources ("Experiments, Text mining, Databases"), a total of 35 ERFE-binding proteins were obtained from the STRING site (<https://string-db.org/>). The protein-protein interaction (PPI) network was visualized using Cytoscape (version 3.7.2). Understanding how proteins interact in biological systems allows us to better understand biological processes like signaling cascades, protein activities, and cellular regulatory mechanisms.

### 2.4. Gene Ontology and Kyoto Encyclopedia of Genes and Genomes enrichment analyses

35 ERFE-binding proteins were subjected to Gene Ontology (GO) and Kyoto Encyclopedia of Genes and Genomes (KEGG) enrichment analyses using the ggplot2 package for visualization and the Cluster Profiler package for statistical analysis [19,20]. GO aids in our understanding and comparison of the functions of genes and proteins in various organisms. KEGG offers a flexible platform for comparative analysis of genomes and metabolic pathways to identify biological processes and pathways associated with specific diseases, which is of great significance for drug design and disease treatment.

### 2.5. Diagnostic value analysis

The pan-cancer diagnostic utility of ERFE was evaluated using a receiver operating characteristic (ROC) curve. It seeks to ascertain whether a test or procedure can identify the existence or absence of a particular illness or condition. The area of the ROC curve ranges from 0.5 to 1. The area under the curve's (AUC) proximity indicated the diagnostic effectiveness. AUC between 0.5 and 0.7 has a poor accuracy; AUC between 0.7 and 0.9 has some accuracy; and AUC over 0.9 has a high accuracy.

### 2.6. Survival prognosis analysis

The correlation between ERFE expression and cancer prognosis (OS, DSS, and PFI) was examined using Kaplan-Meier plots. Additionally, we examined the relationships between ERFE expression and prognosis in several clinical subgroups of COAD patients (OS, DSS, and PFI). The survival package was used for statistical analysis, and the Survminer package was used for visualization. The hypothesis test employed Cox regression, with statistical significance set at  $p < 0.05$ . It can assess patient survival rates and expectations for particular illnesses. This study can be used in clinical research and practice to help medical professionals and researchers better understand patient survival status and establish a foundation for creating individualized treatment strategies for each patient.

### 2.7. Associations between ERFE expression and different clinical characteristics in COAD

Box plots and tables show ERFE expression levels in patients with various clinical features of COAD. The RNA-seq data and corresponding clinical data were downloaded from the TCGA database in level 3 HTSeq-fragments per kilobase per million (FPKM) format. Subsequently, the data were transformed into transcripts per million reads (TPM) format and then log<sub>2</sub>-converted before analysis. Two sets of data were found using the Wilcoxon rank sum test, and statistical significance was determined at  $p < 0.05$  (ns,  $p \geq 0.05$ ; \*,  $p < 0.05$ ; \*\*,  $p < 0.01$ ; \*\*\*,  $p < 0.001$ ).

### 2.8. Univariate and Multivariate Cox regression analyses in COAD

Univariate and multivariate Cox regression analyses were performed to assess the predictive values of ERFE and the clinical features for OS, DSS, and PFI for COAD. Statistical analyses were performed using the Survival program. Multivariate Cox regression analysis further investigated the comprehensive impact of multiple factors and revealed the independent effects of each factor on survival under mutual influence. Univariate Cox regression analysis was used to screen and evaluate the impact of a single factor on survival in a preliminary manner. These analyses assist in identifying and quantifying crucial survival determinants, providing valuable insight for clinical decision-making. This includes the creation of personalized treatment regimens and the prediction of patient survival expectations.

### 2.9. Co-expression gene analysis of ERFE in COAD

We examined at the top 50 genes with ERFE expression in COAD that were both positively and negatively correlated with co-expression. The Stat package was used to display the gene co-expression heatmaps. Using the Pearson correlation coefficient, we also displayed the heatmap's correlations between the expression of the top ten genes and ERFE. It provides crucial insights for researching disease mechanisms, identifying novel therapeutic targets, and developing customized medicines. It also helps us to comprehend the roles and interconnections of genes in biological processes.

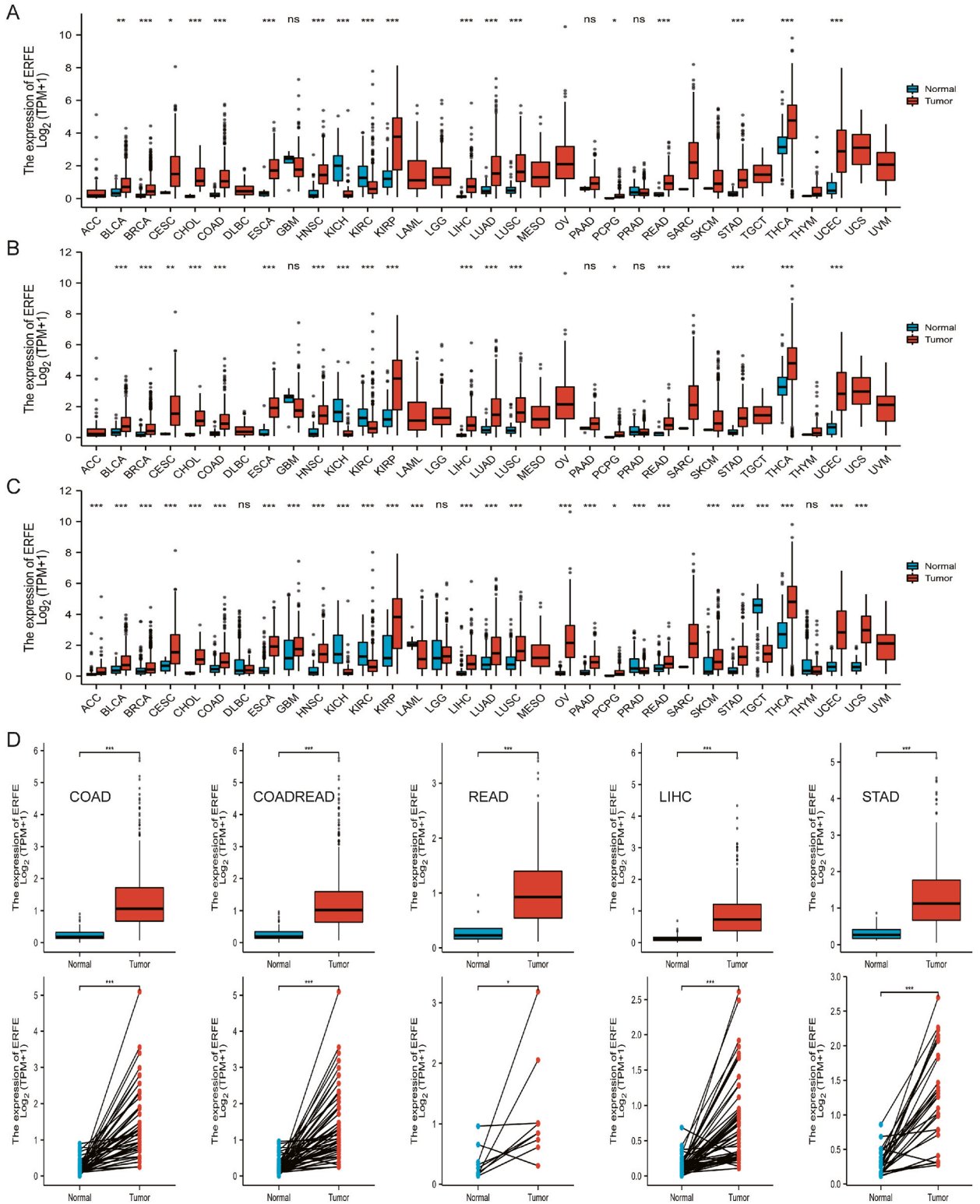


**Fig. 1.** The expression level of ERFE gene in tumor and normal tissues. (A) the expression of ERFE in TCGA tumors and adjacent adjacent tissues; (B) the expression of ERFE in UCSC XENA tumors and adjacent adjacent tissues; (C) the expression of ERFE in UCSC XENA tumors and normal tissues; (D) the expression of ERFE gene in COAD, COADREAD, READ, LIHC and STAD of TCGA (ns,  $p \geq 0.05$ ; \*,  $p < 0.05$ ; \*\*,  $p < 0.01$ ; \*\*\*,  $p < 0.001$ ).

### 2.10. Analysis of immune cell infiltration

To examine the expression levels of genes expression in the published list of distinctive genes, we assessed the relative tumor invasion levels of 24 different immune cell types were assessed using ssGSEA [21]. We investigated the association between ERFE and the degree of immune cell infiltration using Pearson's correlation and other techniques. It can assess the properties of immune cells in tumor tissues, forecast patient survival and treatment efficacy, identify immune escape routes and direct immunotherapy tactics, and comprehend the immunological features of the tumor microenvironment. These capabilities provide crucial data for the development of tailored treatment plans and immunotherapeutic strategies.

## 3. Result

### 3.1. Expression of ERFE in pan-cancer

A study of tumors in the TCGA database showed that ERFE expression was significantly up-regulated in 20 cancer types, including Bladder Urothelial Carcinoma (BLCA), Breast invasive carcinoma (BRCA), Cervical squamous cell carcinoma and endocervical adenocarcinoma (CESC), Cholangiocarcinoma (CHOL), COAD, Esophageal carcinoma (ESCA), Head and Neck squamous cell carcinoma (HNSC), Kidney renal papillary cell carcinoma (KIRP), LIHC, Lung adenocarcinoma (LUAD), Lung squamous cell carcinoma (LUSC), Pancreatic adenocarcinoma (PAAD), Pheochromocytoma and Paraganglioma (PCPG), Rectum adenocarcinoma (READ), Sarcoma (SARC), Skin Cutaneous Melanom (SKCM), STAD, Thyroid carcinoma (THCA), Thymoma (THYM) and Uterine Corpus Endometrial Carcinoma (UCEC). Glioblastoma multiforme (GBM), Kidney Chromophobe (KICH), Kidney renal clear cell carcinoma (KIRC), and Prostate adenocarcinoma (PRAD) were also downregulated (Fig. 1A). The expression of ERFE in several cancer types was almost identical to that in TCGA data for UCSCXENA tumors and surrounding paracancerous tissues (Fig. 1B). For UCSCXENA tumors and adjacent normal tissues, ERFE expression was significantly up-regulated in eight cancer types, including: Adrenocortical carcinoma (ACC), BLCA, BRCA, CESC, CHOL, COAD, ESCA, GBM, HNSC, KIRP, LIHC, LUAD, LUSC, Ovarian serous cystadenocarcinoma (OV), PAAD, PCPG, READ, SKCM, STAD, THCA, UCEC and Uterine Carcinosarcoma (UCS). It was found to be down-regulated in KICH, KIRC, PRAD, and Testicular Germ Cell Tumors (TGCT) (Fig. 1C). The unmatched samples were then compared with paired samples of gastrointestinal tumors. As shown in Fig. 1D, the expression of ERFE expression significantly increased in the following cancers: COAD, COADREAD, READ, LIHC, and STAD. The upper and lower panels compare unmatched and paired samples, respectively. We focused on examining the differential expression of ERFE in colon cancer cell lines. The results showed that ERFE mRNA expression was significantly enhanced in colon cancer cell lines. This study suggests that the differential expression of ERFE may be associated with the occurrence and progression of colon cancer (Fig. 2).

### 3.2. PPI network and GO and KEGG enrichment analyses

We evaluated 35 ERFE-targeted binding proteins using the STRING database and the Cytoscape software (Fig. 3A). We then performed a GO enrichment analysis on 35 targeted binding proteins (Fig. 3B), which revealed that the primary biological processes (BP) included cellular transition metal ion homeostasis, iron ion homeostasis, and cellular iron ion homeostasis. Cellular components (CC) are primarily composed of the cell cortex, recycled endosomes, and collagen trimers. The enrichment of KEGG pathways (Fig. 3C) was primarily related to hematopoietic cell lineage, ferroptosis, and mineral absorption.

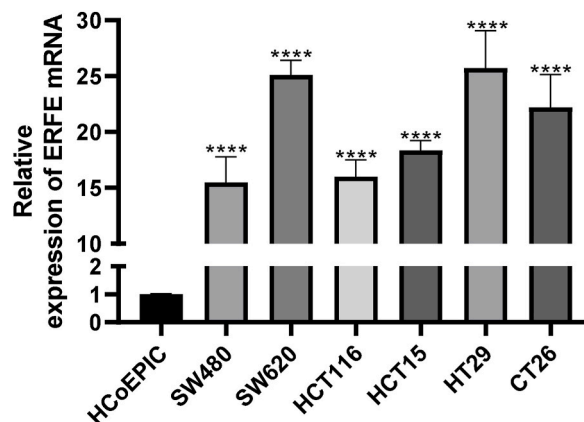


**Fig. 2.** Validation of differential expression of ERFE.

Expression levels in normal human colon epithelial cells (HCoEPIC) and colon cancer cells (SW480, SW620, HCT116, HCT15, HT29, and CT26) were determined using RT-qPCR. Data are expressed as mean  $\pm$  standard deviation. Student's t-test, \*\*\*\*P < 0.0001, compared with the HCoEPIC groups.

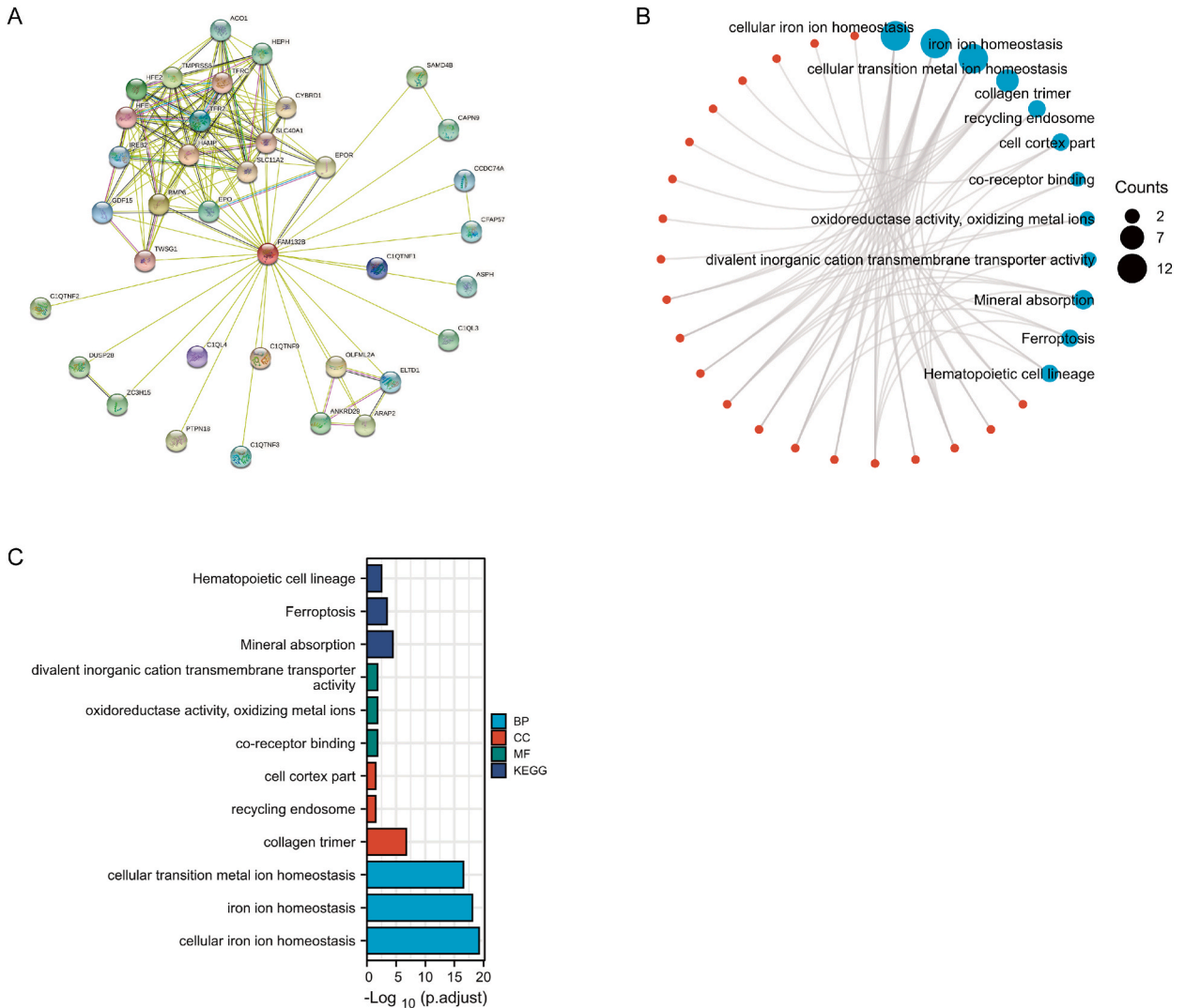


**Fig. 3.** ERFE's protein-protein interaction (PPI) network, GO analysis, and KEGG analysis of 35 targeted binding proteins. (A) PPI network; (B) visual network of GO and KEGG analysis; (C) GO analysis and KEGG analysis.

### 3.3. Prognostic value of ERFE in cancer

Particularly in LIHC, COAD, STAD, and COADREAD, ERFE expression was substantially linked to OS, DSS and PFI in digestive tract cancers. According to the findings of LIHC and Cox regression analyses, patients with high ERFE expression had a worse prognosis. Including OS (HR = 1.67, 95% CI: 1.17–2.39,  $p = 0.005$ ; Fig. 4A), DSS (HR = 1.96, 95% CI: 1.24–3.11,  $p = 0.004$ ; Fig. 4B), and PFI (HR = 1.60, 95% CI: 1.20–2.14,  $p = 0.002$ ; Fig. 4C). Further, COAD, Cox regression results revealed that patients with high ERFE expression had a worse prognosis for OS (HR = 2.32, 95% CI: 1.57–3.41,  $p < 0.001$ ; Fig. 4D), DSS (HR = 2.74, 95% CI: 1.67–4.48,  $p < 0.001$ ; Fig. 4E), and PFI (HR = 2.01, 95% CI: 1.41–2.84,  $p < 0.001$ ; Fig. 4F). According to STAD and Cox regression findings, patients with high ERFE expression had a worse prognosis for OS (HR = 1.71, 95% CI: 1.11–2.64,  $p = 0.015$ ), DSS (HR = 1.69, 95% CI: 0.98–2.91,  $p = 0.057$ ), and PFI (HR = 1.58, 95% CI: 1.02–2.48,  $p = 0.042$ ) (Fig. 4G-I). According to the COADREAD, Cox regression results, patients with high levels of ERFE had a worse prognosis for their conditions, including OS (HR = 1.98, 95% CI: 1.40–2.81,  $p < 0.001$ ), DSS (HR = 2.40, 95% CI: 1.54,  $p < 0.001$ ), and PFI (HR = 1.92, 95% CI: 1.41–2.62,  $p < 0.001$ ) (Fig. 4J-L).

Furthermore, we introduced the relationship between ERFE and different clinical features of COAD (Table 1) and investigated the relationship between ERFE and prognosis (OS, DSS, and PFI) in different clinical subgroups of COAD. The results showed that high ERFE expression was associated with poor OS in the majority of clinical subgroups, whether in the age = 65 years old or >65 years old subgroup (Fig. 5A-B), gender subgroup (Fig. 5C-D), T stage:T3 and T4 subgroup (Fig. 5F), N stage:N0 subgroup (Fig. 5G), M stage:M0 subgroup (Fig. 5H), Pathologic stage:Stage I and II subgroup and Stage III and IV subgroup (Fig. 5I-J). The high expression of DSS and ERFE was comparable to that of OS, and there was poorer DSS in the subgroups of age = 65 or >65 years old, gender, T stage:T3 and T4

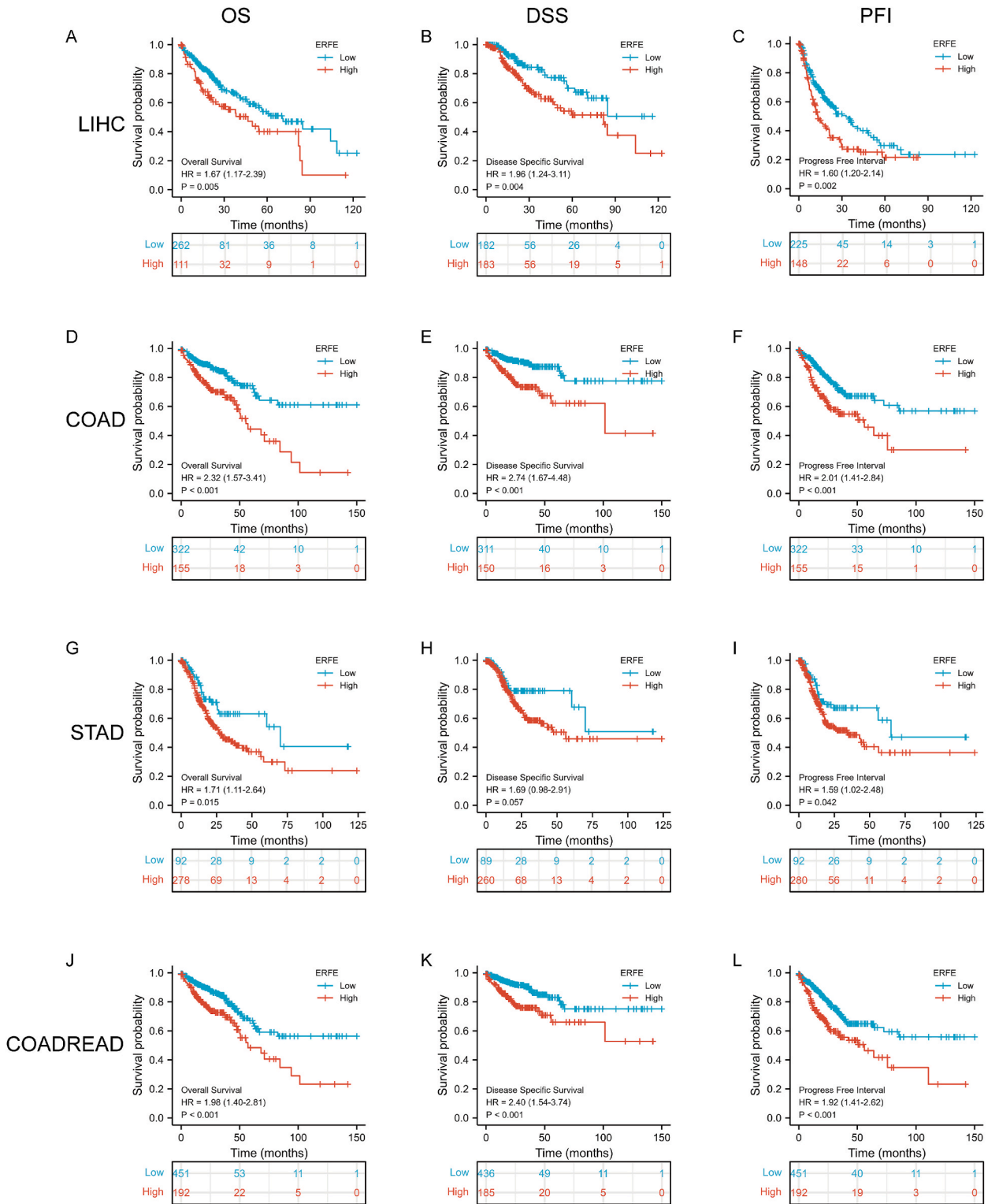


**Fig. 4.** Correlations between ERFE expression and the prognosis (OS, DSS, and PFI) of cancers. (A–C) LIHC; (D–F) COAD; (G–I) STAD; (J–L) COADREAD.

**Table 1**  
The relationship between ERFE and different clinical features of COAD.

Characteristic	Low expression of ERFE	High expression of ERFE	p
n	239	239	
T stage, n (%)			0.049
T1	9 (1.9%)	2 (0.4%)	
T2	48 (10.1%)	35 (7.3%)	
T3	151 (31.7%)	172 (36.1%)	
T4	30 (6.3%)	30 (6.3%)	
N stage, n (%)			0.356
N0	147 (30.8%)	137 (28.7%)	
N1	55 (11.5%)	53 (11.1%)	
N2	37 (7.7%)	49 (10.3%)	
M stage, n (%)			0.337
M0	170 (41%)	179 (43.1%)	
M1	37 (8.9%)	29 (7%)	
Pathologic stage, n (%)			0.140
Stage I	47 (10.1%)	34 (7.3%)	
Stage II	90 (19.3%)	97 (20.8%)	
Stage III	58 (12.4%)	75 (16.1%)	
Stage IV	37 (7.9%)	29 (6.2%)	
Primary therapy outcome, n (%)			0.054
PD	8 (3.2%)	17 (6.8%)	
SD	4 (1.6%)	0 (0%)	
PR	7 (2.8%)	6 (2.4%)	
CR	108 (43.2%)	100 (40%)	
Gender, n (%)			0.410
Female	118 (24.7%)	108 (22.6%)	
Male	121 (25.3%)	131 (27.4%)	
Race, n (%)			0.109
Asian	4 (1.3%)	7 (2.3%)	
Black or African American	39 (12.7%)	24 (7.8%)	
White	113 (36.9%)	119 (38.9%)	
Age, n (%)			0.113
≤65	106 (22.2%)	88 (18.4%)	
>65	133 (27.8%)	151 (31.6%)	
Weight, n (%)			0.261
≤90	97 (35.5%)	92 (33.7%)	
>90	50 (18.3%)	34 (12.5%)	
Height, n (%)			0.714
<170	66 (25.8%)	61 (23.8%)	
≥170	71 (27.7%)	58 (22.7%)	
BMI, n (%)			0.181
<25	41 (16%)	46 (18%)	
≥25	96 (37.5%)	73 (28.5%)	
Residual tumor, n (%)			0.733
R0	174 (46.5%)	172 (46%)	
R1	1 (0.3%)	3 (0.8%)	
R2	12 (3.2%)	12 (3.2%)	
CEA level, n (%)			1.000
≤5	100 (33%)	96 (31.7%)	
>5	55 (18.2%)	52 (17.2%)	
Perineural invasion, n (%)			0.635
NO	72 (39.8%)	63 (34.8%)	
YES	22 (12.2%)	24 (13.3%)	
Lymphatic invasion, n (%)			1.000
NO	132 (30.4%)	134 (30.9%)	
YES	84 (19.4%)	84 (19.4%)	
History of colon polyps, n (%)			0.964
NO	133 (32.6%)	129 (31.6%)	
YES	73 (17.9%)	73 (17.9%)	
Colon polyps present, n (%)			0.419
NO	83 (33.3%)	79 (31.7%)	
YES	50 (20.1%)	37 (14.9%)	
Neoplasm type, n (%)			1.000
Colon adenocarcinoma	239 (50%)	239 (50%)	
Rectum adenocarcinoma	0 (0%)	0 (0%)	
OS event, n (%)			0.004
Alive	201 (42.1%)	174 (36.4%)	
Dead	38 (7.9%)	65 (13.6%)	
DSS event, n (%)			0.003

(continued on next page)

**Table 1** (continued)

Characteristic	Low expression of ERFE	High expression of ERFE	p
Alive	209 (45.2%)	189 (40.9%)	0.018
Dead	20 (4.3%)	44 (9.5%)	
PFI event, n (%)			0.009
Alive	187 (39.1%)	163 (34.1%)	
Dead	52 (10.9%)	76 (15.9%)	
Age, median (IQR)	68 (56.5, 75)	70 (60.5, 79)	

subgroup, N stage:N0 subgroup, M stage:M0 subgroup, Pathologic stage:Stage I and II subgroup and Stage III and IV subgroup (Fig. 6). There was no difference in the Gender:Female subgroup (Fig. 7A-D), but there was a worse PFI in the T stage:T1 and T2 subgroup, which is the difference between the high expression of PFI, OS, and DSS (Fig. 7E-J).

### 3.4. The diagnostic value of ERFE in pan-cancer

To assess the pan-cancer diagnostic utility of ERFE, an ROC curve was constructed. These results support the hypothesis. ERFE showed a high degree of accuracy in predicting nine different forms of cancer (Fig. 8), with an AUC higher than 0.9, and was more accurate at predicting cancers of the digestive tract than LIHC (AUC = 0.947) (Fig. 8A), COAD (AUC = 0.942) (Fig. 8B), COADREAD (AUC = 0.931) (Fig. 8C) and STAD (AUC = 0.912) (Fig. 8D). Also, we looked at the correlation between ERFE and subject operating characteristic (ROC) curves in several clinical subgroups of COAD to determine their diagnostic usefulness. Except for T stage:T1 (AUC = 0.858) (Fig. 9E), the data demonstrated that ERFE had great accuracy in predicting several clinical subgroups (AUC ≥ 0.92) (Fig. 9A-D, F-Q).

### 3.5. Analysis of co-expression genes of ERFE in COAD

Figs. 10A and 11A show the top 50 genes that were positively or negatively correlated with ERFE expression in patients with COAD (Figs. 10–11). The scatter plot shows the top ten positively or negatively correlated co-expressed genes: C19orf38 ( $r = 0.460$ ) in Fig. 10B, FBXL16 ( $r = 0.448$ ) in Fig. 10C, ELOVL3 ( $r = 0.443$ ) in Fig. 10D, C2CD4C ( $r = 0.421$ ) in Fig. 10E, and ULBP2 ( $r = 0.420$ ) in Fig. 10F. AC124067.4 ( $r = -0.397$ ) in Fig. 11B, LY6G6D ( $r = -0.375$ ) in Fig. 11C, ACE2 ( $r = -0.373$ ) in Fig. 11D, CTTNBP2 ( $r = -0.372$ ) in Fig. 11E, and VAV3 ( $r = -0.369$ ) in Fig. 11F.

### 3.6. Analysis of correlation between the ERFE gene and different immune cells in COAD

We investigated this relationship using Pearson's correlation analysis between the level of infiltration of 24 different types of immune cells as measured by ssGSEA and the expression level of ERFE in COAD (TPM). The findings demonstrated that the expression of ERFE was negatively connected with the abundance of Tcm (T central memory) and positively correlated with the abundance of Cytotoxic cells, Th1 cells, and aDC (activated DC). According to these findings, ERFE might be crucial for the immunological infiltration of COAD (Fig. 12A-K,  $P < 0.001$ ).

## 4. Discussion

Having previously been categorized as C1q/TNF-related protein 15 (CTRP15), and myonectin [8], erythroferrone (ERFE), and Family32b before renaming [4–7], a significant role in regulating ferritin and iron homeostasis has recently been demonstrated. Many recent studies have clarified its relationship with atherosclerosis, myocardial fibrosis, insulin resistance, ulcerative colitis, and dyslipidemia [22–28]. A recent study confirmed the important role of ERFE in cancer cachexia and skeletal muscle atrophy [29]. To the best of our knowledge, iron-related illnesses continue to be the primary focus of contemporary research. Research on the relationship between ERFE and cancer, which is crucial for the effective augmentation of ERFE, is still lacking. In this study, we first assessed the pan-cancer ERFE expression levels. In our database, we discovered in our database that 20 different cancer types showed considerably higher ERFE expression levels. It includes BLCA, BRCA, CESC, CHOL, COAD, ESCA, HNSC, KIRP, LIHC, LUAD, LUSC, PAAD, PCPG, READ, SARC, SKCM, STAD, THCA, THYM, and UCEC and is down-regulated in GBM, KICH, KIRC and PRAD. These results imply that ERFE functions as an oncogene in most malignant tumors and is probably involved in carcinogenesis or the emergence of cancer. Furthermore, we found that the gastrointestinal cancer we chose had a markedly elevated expression of ERFE, which strongly suggests a unique correlation between ERFE and gastrointestinal malignancies. We also validated this with a variety of colon cancer cell lines. The primary biological process (BP), encompassing cellular transition metal ion homeostasis, iron ion homeostasis, and cellular iron ion homeostasis, were subsequently enriched and evaluated using 35 targeted binding proteins of ERFE. The cell cortical portion, recycling endosomes, and collagen trimers comprise the majority of the cellular components (CC). Ironoptosis, mineral absorption, and hematopoietic cell lineage were the three main topics of the KEGG pathway enrichment.

The diagnostic and prognostic utility of ERFE in digestive tract cancers was next evaluated. ERFE expression was significantly associated with OS, DSS, and PFI in digestive tract cancers, particularly LIHC, COAD, STAD, and COADREAD, according to the Kaplan-Meier survival curve. We also examined the relationship between ERFE expression levels and age, sex, stage, histological grade, and

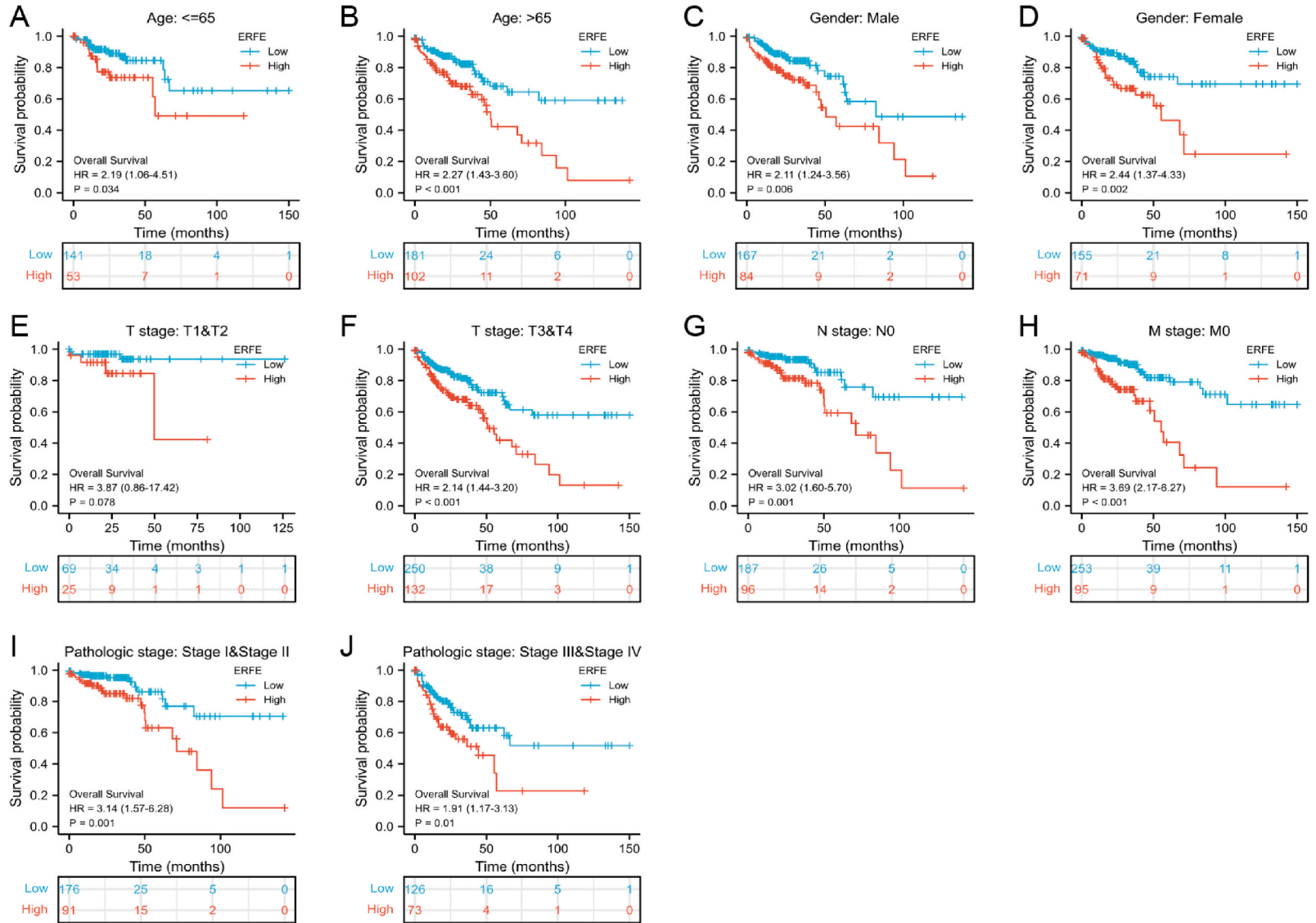


**Fig. 5.** The correlation between ERFE expression and OS in the different clinical subgroups of COAD. (A,B)Age subgroup; (C,D)Gender subgroup; (E-H)TNM stage subgroup; (I,J)Pathologic stage subgroup.

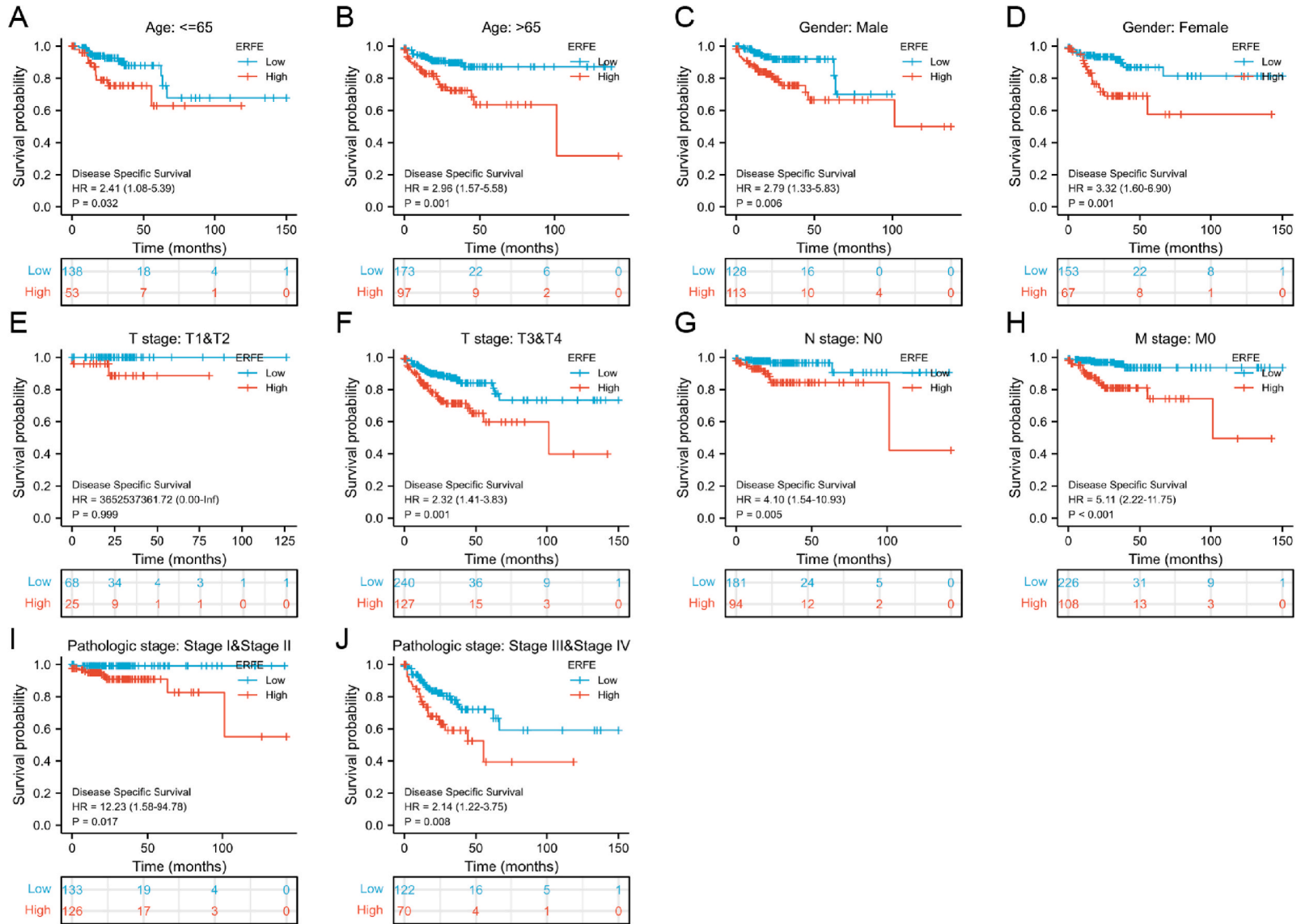


**Fig. 6.** The correlation between ERFE expression and DSS in different clinical subgroups of COAD. (A,B)Age subgroup; (C,D)Gender subgroup; (E-H)TNM stage subgroup; (I,J)Pathologic stage subgroup.

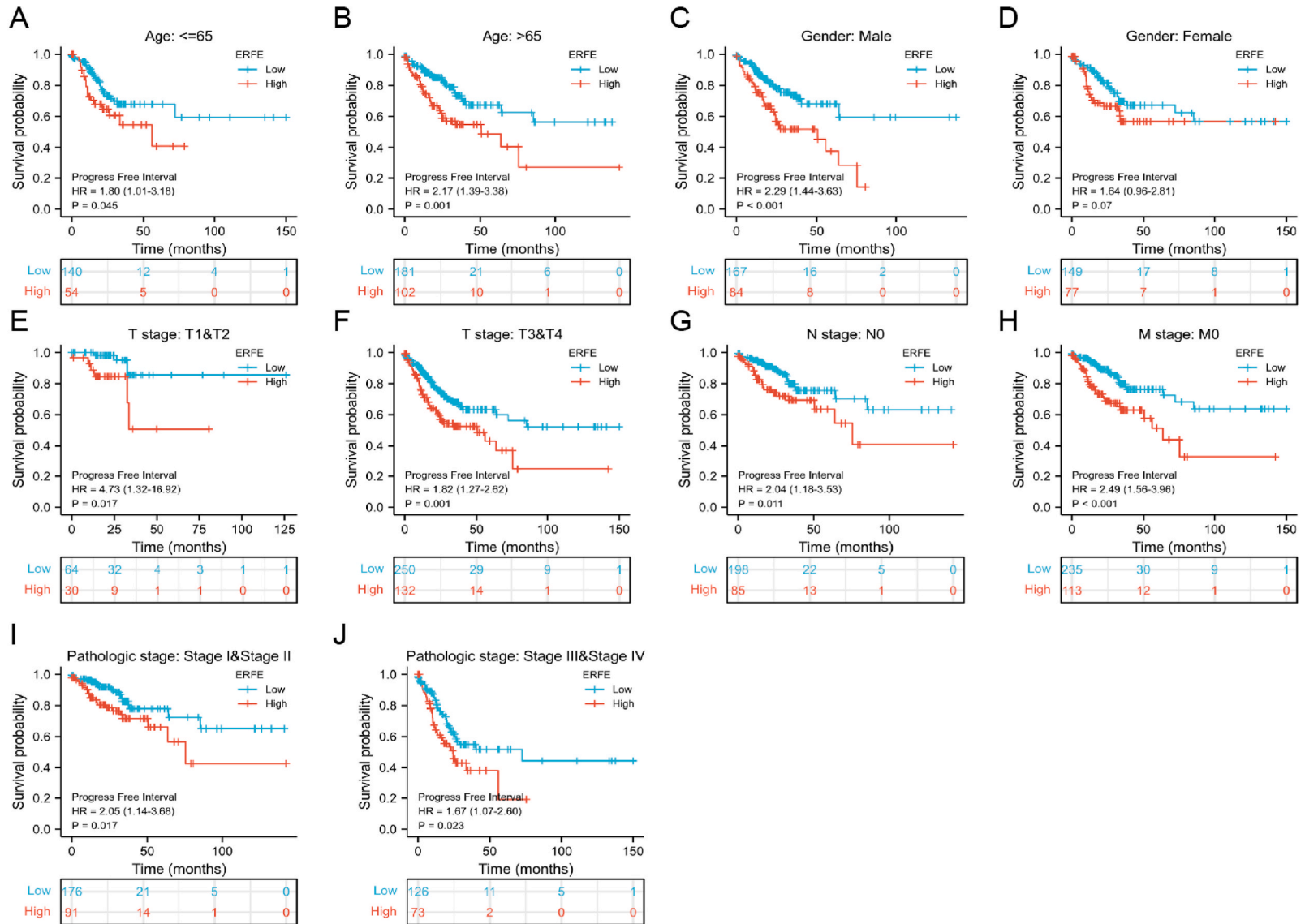


**Fig. 7.** The correlation between ERFE expression and PFI in different clinical subgroups of COAD. (A,B)Age subgroup; (C,D)Gender subgroup; (E-H)TNM stage subgroup; (I,J)Pathologic stage subgroup.

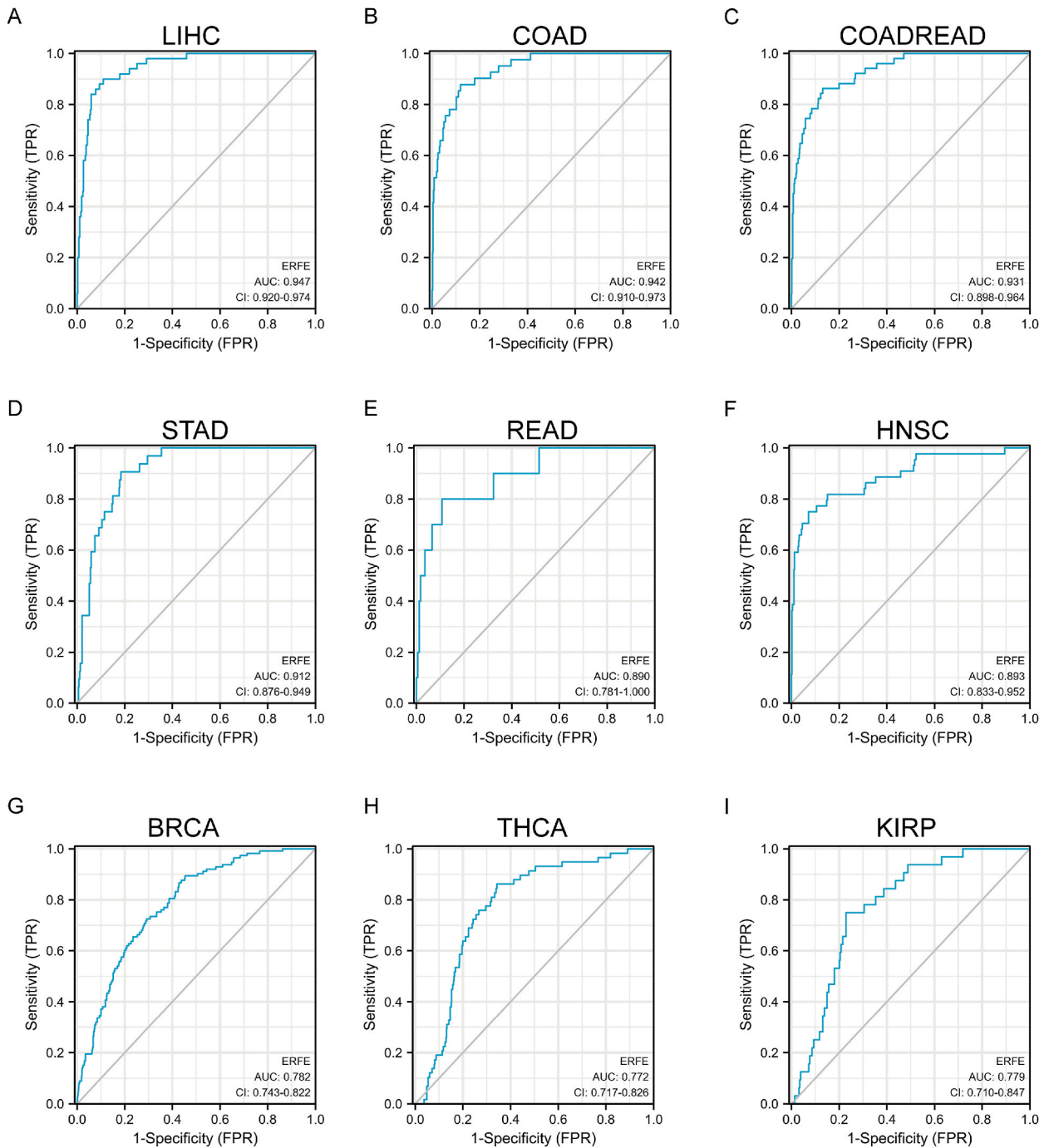


**Fig. 8.** Receiver operating characteristic (ROC) curve for ERFE expression in pan-cancer. (A)LIHC; (B) COAD; (C)COADREAD; (D)STAD; (E) READ; (F) HNSC; (G)BRCA; (H)THCA; (I)KIRP.

prognosis (OS, DSS, and PFI) in various clinical subgroups of COAD ( Table 1 ). According to the ROC curve data, ERFE accurately identified nine different cancer types. Among these, LIHC, COAD, COADREAD, and STAD exhibited the highest accuracy for predicting digestive tract cancer (AUC >0. 9). Therefore, we focused on the diagnostic utility of ERFE and subject operating characteristic (ROC) curves in various clinical subgroups of COAD. The findings showed that, with the exception of Tstage:T1 (AUC = 0.858), ERFE had high accuracy in predicting other clinical subgroups (AUC >0.9). These findings demonstrate the diagnostic and prognostic importance of ERFE in malignancies, particularly in gastrointestinal cancers, and suggest that ERFE may be a viable biomarker or therapeutic target for precision oncology. We analyzed the ERFE and clinical characteristics of COAD using univariate and multivariate Cox

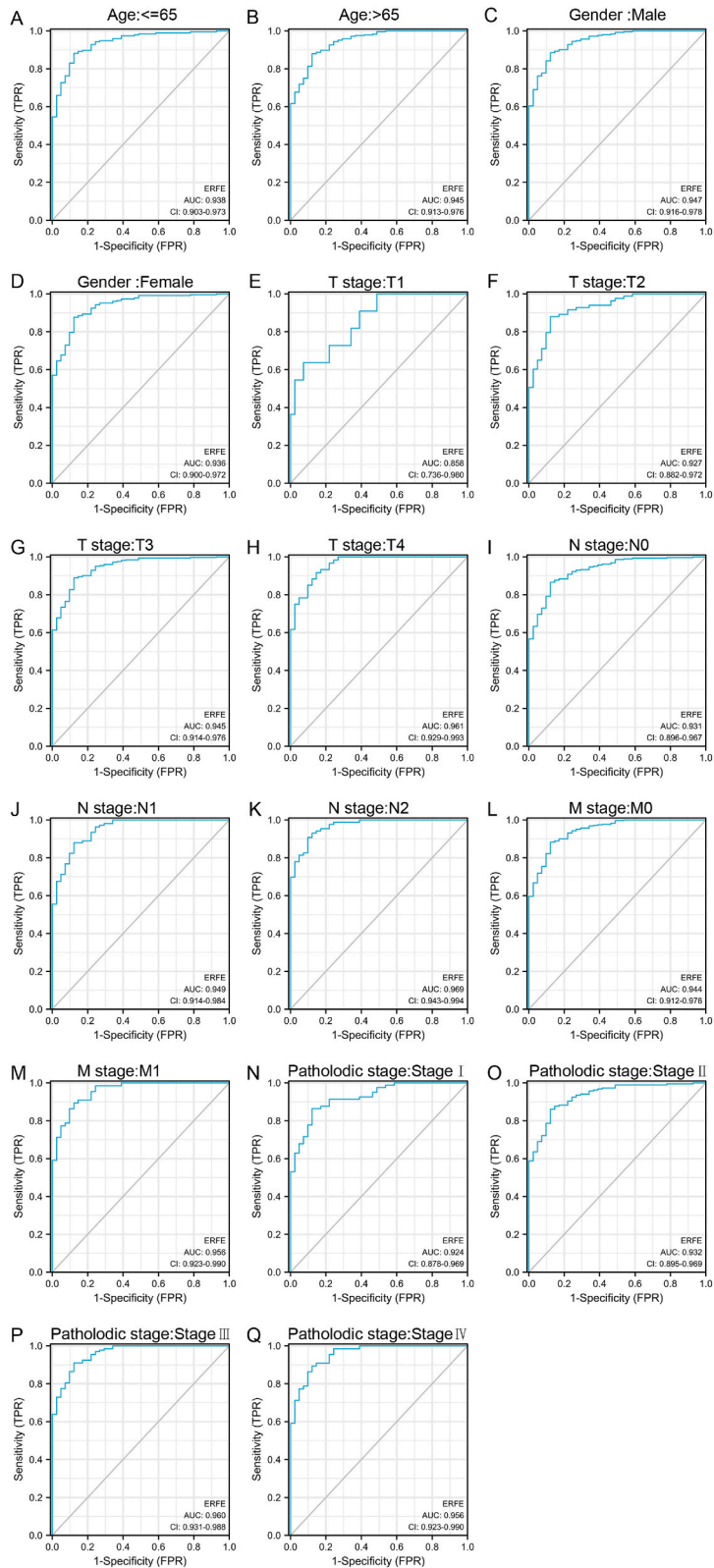


**Fig. 9.** ERFE has a high accuracy in predicting different clinical subgroups of COAD. (A,B)Age subgroup; (C,D)Gender subgroup; (E-M)TNM stage subgroup; (N-Q)Pathologic stage subgroup.

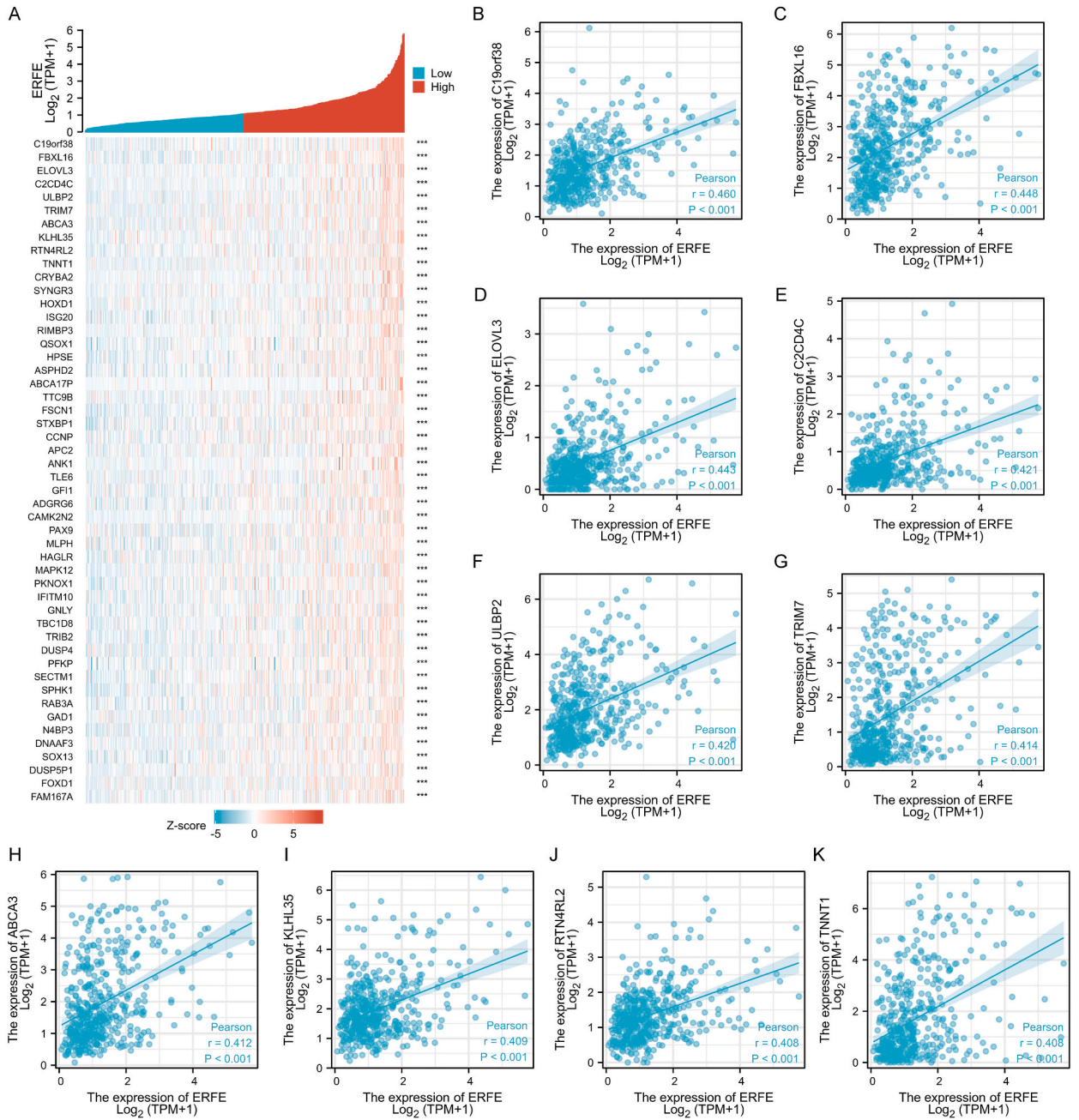


**Fig. 10.** The top 50 genes positively correlated with ERFE expression in COAD.

(A) The gene co-expression heatmap of the top 50 genes positively correlated with ERFE in CAOD; (B–K) Correlation analysis of the top 10 genes and ERFE in the heatmap.

regression analyses. Clinical stage, pathologic stage, primary therapeutic outcome, and fe were strongly associated with OS in univariate and multivariate Cox regression analyses (Supplementary Table 1). These associations were consistent with the results observed for DSS (Supplementary Table 2) and PFI (Supplementary Table 3).

We used COAD as an example to examine the potential genes co-expressed with ERFE. C19orf38, FBXL16, ELOVL3, C2CD4C, ULBP2, TRIM7, ABCA3, KLHL35, RTN4RL2, and TNNT1 were the top ten positively connected genes. In contrast, AC124067.4, LY6G6D, ACE2, CTTNBP2, VAV3, TINAG, LY6G6F-LY6G6D, SLC39A5, PRR15, and A1CF negatively correlated with ERFE. Additionally, we performed a correlation analysis between the ERFE gene and various immune cells in COAD. This analysis revealed a significant positive correlation between cytotoxic cells, Th1 cells, aDC, and other cells, but a negative correlation with Tcm cells, indicating that ERFE may also be a key player in tumor immune infiltration. This study offers a tremendous opportunity to deepen our

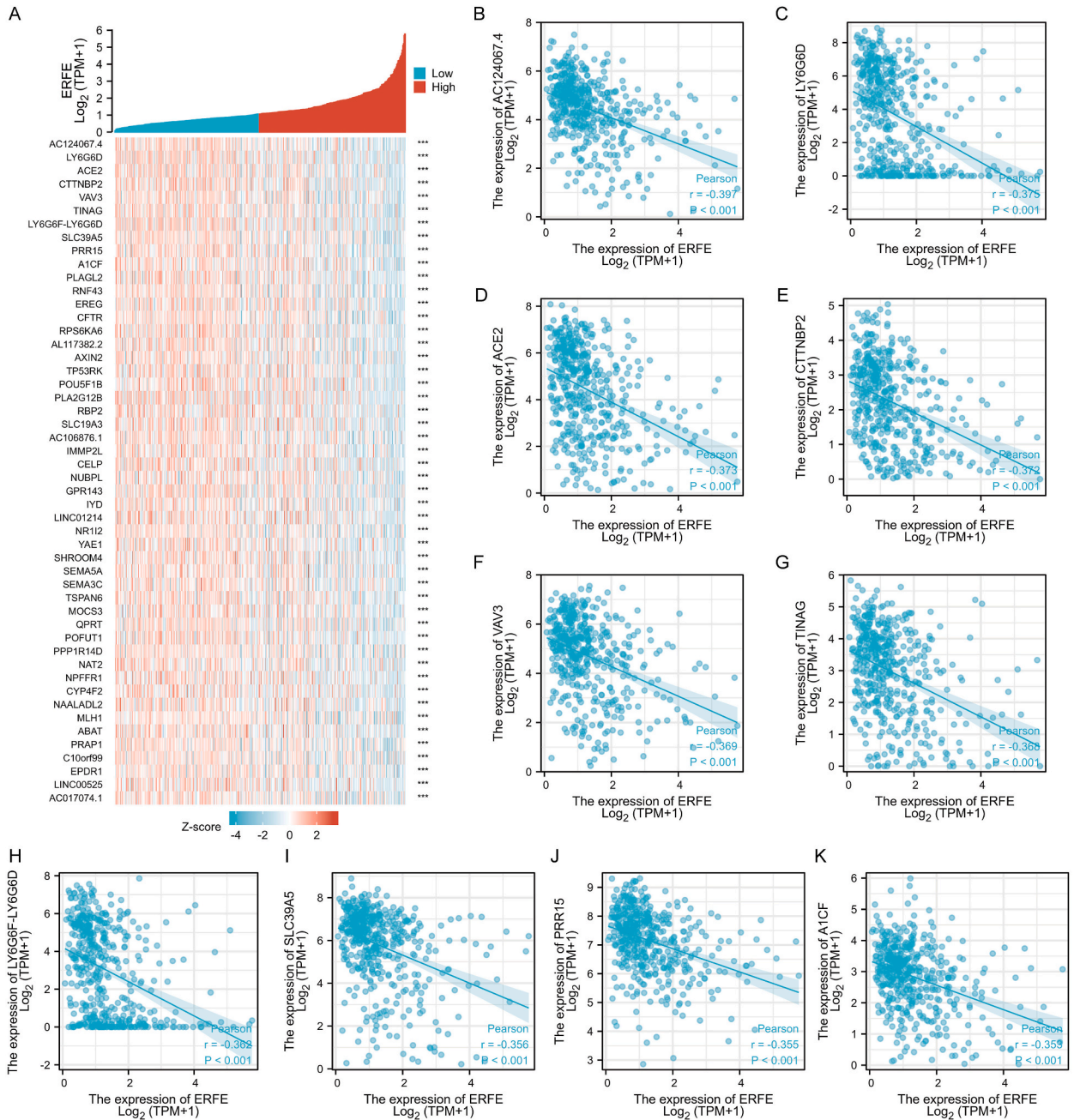


**Fig. 11.** The top 50 genes negatively correlated with ERFE expression in COAD. (A) The gene co-expression heatmap of the top 50 genes negatively correlated with ERFE in CAOD; (B–K) Correlation analysis of the top 10 genes and ERFE in the heatmap.

understanding of ERFE, which could pave the way for personalized treatments in the future. Thus, treatment adjustments can be tailored to each patient’s unique situation, resulting in more accurate and effective outcomes. Furthermore, the function of ERFE as a molecular biomarker may contribute to the development of precise cancer screening tools, enabling the early detection and treatment of cancer. Our research revealed the involvement of ERFE in various types of cancer, highlighting potential new targets for drug development. This study lays a strong foundation for the development of innovative drugs targeting ERFE, which have immense potential to revolutionize cancer treatment. Additionally, ERFE is closely linked to cancer prognosis and may prove to be vital for evaluating patient outcomes. Our research will empower doctors to gain a better understanding of their patient’s conditions and the ability to devise more effective treatment plans. Overall, our findings are poised to propel cancer treatment towards a future of precision, personalized care, and early intervention, providing greater hope and opportunities for patients.

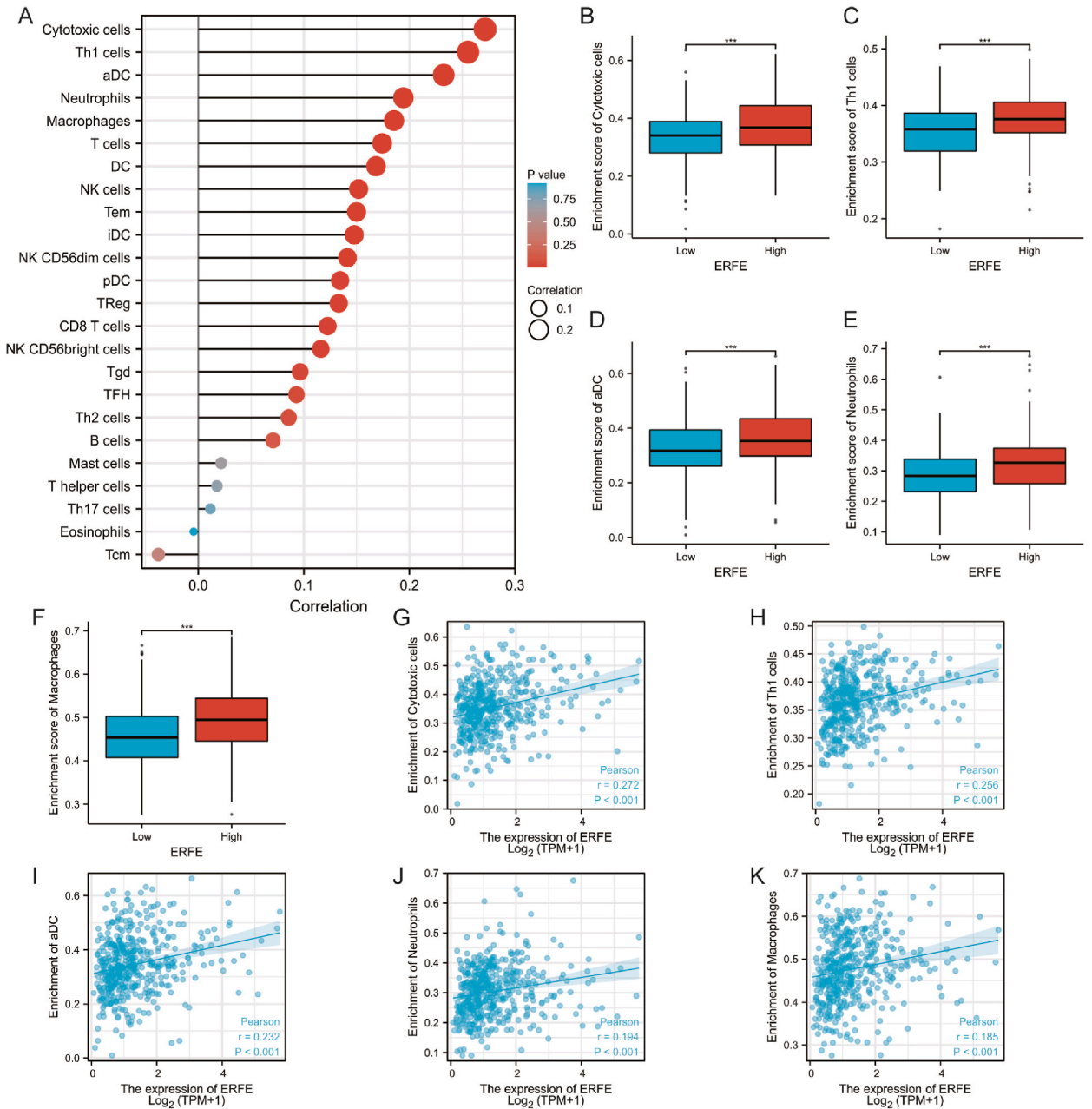


**Fig. 12.** The expression level of ERFE is related to immune infiltration in tumor microenvironment. (A) Correlation analysis between markers and ERFE of 24 kinds of immune cells in COAD, the size of the dot showed the absolute value of Pearson; (B–F) the grouping comparison of the high and low expression of ERFE in the first five immune cells markers; (G–K) the scatter plot of ERFE and the first five immune cells markers. (ns,  $p \geq 0.05$ ; \*,  $p < 0.05$ ; \*\*,  $p < 0.01$ ; \*\*\*,  $p < 0.001$ ).

Of course, it cannot be denied that this study still has certain flaws. On the one hand, due to a lack of actual clinical data, we started using only a few public relations databases to retrieve and analyze ERFE. Further biological tests should be conducted to provide high-quality verification and evidence. The next stage is to conduct high-quality experiments that will yield results that are powerful and significant for this study in order to obtain more trustworthy information. Other bioinformatics techniques are also being investigated, including the prediction of lncRNA-miRNA interactions [30–32], the development of microRNA combination biomarkers [33–35], and others [36,37]. The usage of deep learning [38,39], machine learning techniques [40], and material technology [41–44] in ERFE research will be discussed in the following stage.

## 5. Conclusions

In other words, the discovery of ERFE's importance in the diagnosis and prognosis of pan-cancer, along with its subsequent investigation in COAD, can add a new dimension and provide a thorough analytical foundation for a thorough knowledge of its crucial function in tumor promotion and inhibition. Future clinical applications for the treatment of cancer will result from the thorough validation of more molecular biology investigations.

### Funding

This project was supported by Fujian Provincial Natural Science Foundation ( 2021J011329 ), the Medical Health Science and Technology Project of Xiamen (3502Z20209026), and the Project of Young and Middle-aged Backbone Talents Cultivation, Fujian, China (2022GGB011).

### Availability of data and materials

The data are included in the article/supp. materials/referenced in article.

### Ethics approval and consent to participate

The research in this article does not involve the ethical part, and does not touch on animal experiments and human.

### Consent for publication

Not applicable.

### CRedit authorship contribution statement

**Ying Cai:** Data curation, Conceptualization. **Yaling Gao:** Data curation. **Yinyin Lv:** Formal analysis. **Zhiyuan Chen:** Formal analysis. **Lingfeng Zhong:** Software, Resources. **Junjie Chen:** Software, Resources. **Yanyun Fan:** Writing – review & editing, Writing – original draft, Visualization, Validation, Supervision, Project administration, Funding acquisition.

### Declaration of competing interest

The authors declare that they have no known competing financial interests or personal relationships that could have appeared to influence the work reported in this paper.

### Acknowledgements

Not applicable.

### Appendix A. Supplementary data

Supplementary data to this article can be found online at <https://doi.org/10.1016/j.heliyon.2024.e26990>.

### Abbreviations

Erythroferrone	ERFE
ACC	Adrenocortical carcinoma
BLCA	Bladder Urothelial Carcinoma
BRCA	Breast invasive carcinoma
CESC	Cervical squamous cell carcinoma and endocervical adenocarcinoma
CHOL:	Cholangiocarcinoma
COAD	Colon adenocarcinoma
COADREAD	Colon adenocarcinoma/Rectum adenocarcinoma Esophageal carcinoma
DLBC	Lymphoid Neoplasm Diffuse Large B-cell Lymphoma
ESCA	Esophageal carcinoma
GBM	Glioblastoma multiforme
HNSC	Head and Neck squamous cell carcinoma
KICH	Kidney Chromophobe
KIRC	Kidney renal clear cell carcinoma
KIRP	Kidney renal papillary cell carcinoma

LAML:	Acute Myeloid Leukemia
LGG	Brain Lower Grade Glioma
LIHC	Liver hepatocellular carcinoma
LUAD	Lung adenocarcinoma
LUSC:	Lung squamous cell carcinoma
MESO	Mesothelioma
OV	Ovarian serous cystadenocarcinoma
PAAD	Pancreatic adenocarcinoma
PCPG	Pheochromocytoma and Paraganglioma
PRAD	Prostate adenocarcinoma
READ	Rectum adenocarcinoma
SARC	Sarcoma
SKCM	Skin Cutaneous Melanoma
STAD	Stomach adenocarcinoma
TGCT	Testicular Germ Cell Tumors
THCA	Thyroid carcinoma
THYM	Thymoma
UCEC	Uterine Corpus Endometrial Carcinoma
UCS:	Uterine Carcinosarcoma
UVM	Uveal Melanoma

## References

- [1] D.N. Srole, T. Ganz, Erythroferrone structure, function, and physiology: iron homeostasis and beyond, *J. Cell. Physiol.* 236 (7) (2021) 4888–4901.
- [2] E. Nemeth, M.S. Tuttle, J. Powelson, M.B. Vaughn, A. Donovan, D.M. Ward, et al., Hepcidin regulates cellular iron efflux by binding to ferroportin and inducing its internalization, *Science* 306 (5704) (2004) 2090–2093.
- [3] E. Gammella, V. Diaz, S. Recalcati, P. Buratti, M. Samaja, S. Dey, et al., Erythropoietin's inhibiting impact on hepcidin expression occurs indirectly, *Am. J. Physiol. Regul. Integr. Comp. Physiol.* 308 (4) (2015) R330–R335.
- [4] H. Meng, Y. Yu, E. Xie, Q. Wu, X. Yin, B. Zhao, et al., Hepatic HDAC3 regulates systemic iron homeostasis and ferroptosis via the Hippo signaling pathway, *Research* 6 (2023) 281.
- [5] L. Kautz, G.C. Jung, E.V. Valore, S. Rivella, E. Nemeth, T. Ganz, Identification of erythroferrone as an erythroid regulator of iron metabolism (vol 18, pg 304, 2014), *Nat. Genet.* 52 (4) (2020) 463.
- [6] A.L. Fisher, E. Nemeth, Iron homeostasis during pregnancy, *Am. J. Clin. Nutr.* 106 (6) (2017) 1567S, 74S.
- [7] V. Sangkhae, A.L. Fisher, T. Ganz, E. Nemeth, Iron homeostasis during pregnancy: Maternal, placental, and fetal regulatory mechanisms, *Annu. Rev. Nutr.* 43 (2023) 279–300.
- [8] M.M. Seldin, S.Y. Tan, G.W. Wong, Metabolic function of the CTRP family of hormones, *Rev. Endocr. Metab. Disord.* 15 (2) (2014) 111–123.
- [9] G.W. Wong, J. Wang, C. Hug, T.S. Tsao, H.F. Lodish, A family of Acrp30/adiponectin structural and functional paralogs, *Proc Natl Acad Sci U S A* 101 (28) (2004) 10302–10307.
- [10] F. Ayub, H. Ahmed, T. Sohail, K. Shahzad, F. Celik, X. Wang, et al., Bioinformatics-based prediction and screening of immunogenic epitopes of *Toxoplasma gondii* rhoptry proteins 7, 21 and 22 as candidate vaccine target, *Helv. J. Biol.* 9 (7) (2023).
- [11] N. Blom, T. Sicheritz-Ponten, R. Gupta, S. Gammeltoft, S. Brunak, Prediction of post-translational glycosylation and phosphorylation of proteins from the amino acid sequence, *Proteomics* 4 (6) (2004) 1633–1649.
- [12] Y. Wang, K.S.L. Lam, M.H. Yau, A.M. Xu, Post-translational modifications of adiponectin: mechanisms and functional implications, *Biochem. J.* 409 (2008) 623–633.
- [13] M. Paudel, S. Kaffle, T.R. Gombo, K.B. Khatri, A. Aryal, Microbiological and hematological aspects of canine pyometra and associated risk factors, *Heliyon* 9 (12) (2023) e22368-e.
- [14] V.H. Haase, Regulation of erythropoiesis by hypoxia-inducible factors, *Blood Rev.* 27 (1) (2013) 41–53.
- [15] J. Ferlay, M. Colombet, I. Soerjomataram, C. Mathers, D.M. Parkin, M. Pineros, et al., Estimating the global cancer incidence and mortality in 2018: GLOBOCAN sources and methods, *Int. J. Cancer* 144 (8) (2019) 1941–1953.
- [16] F. Bray, J. Ferlay, I. Soerjomataram, R.L. Siegel, L.A. Torre, A. Jemal, Global cancer statistics 2018: GLOBOCAN estimates of incidence and mortality worldwide for 36 cancers in 185 countries, *CA Cancer J Clin* 68 (6) (2018) 394–424.
- [17] C. Wu, M. Li, H. Meng, Y. Liu, W. Niu, Y. Zhou, et al., Analysis of status and countermeasures of cancer incidence and mortality in China, *Sci. China Life Sci.* 62 (5) (2019) 640–647.
- [18] K.D. Miller, L. Nogueira, A.B. Mariotto, J.H. Rowland, K.R. Yabroff, C.M. Alfano, et al., Cancer treatment and survivorship statistics, *CA Cancer J Clin* 69 (5) (2019) 363–385, 2019.
- [19] S.J. O'Keefe, Diet, microorganisms and their metabolites, and colon cancer, *Nat. Rev. Gastroenterol. Hepatol.* 13 (12) (2016) 691–706.
- [20] A. Subramanian, P. Tamayo, V.K. Mootha, S. Mukherjee, B.L. Ebert, M.A. Gillette, et al., Gene set enrichment analysis: a knowledge-based approach for interpreting genome-wide expression profiles, *Proceedings of the National Academy of Sciences of the United States of America* 102 (43) (2005) 15545–15550.
- [21] G.C. Yu, L.G. Wang, Y.Y. Han, Q.Y. He, clusterProfiler: an R Package for comparing biological themes among gene clusters, *Omics-a Journal of Integrative Biology* 16 (5) (2012) 284–287.
- [22] G. Bindea, B. Mlecnik, M. Tosolini, A. Kirilovsky, M. Waldner, A.C. Obenauf, et al., Spatiotemporal dynamics of intratumoral immune cells reveal the immune landscape in human cancer, *Immunity* 39 (4) (2013) 782–795.
- [23] Q. Mi, Y. Li, M. Wang, G. Yang, X. Zhao, H. Liu, et al., Circulating C1q/TNF-related protein isoform 15 is a marker for the presence of metabolic syndrome, *Diabetes Metab Res Rev* 35 (1) (2019) e3085.
- [24] Q. Zhao, C.L. Zhang, R.L. Xiang, L.L. Wu, L. Li, CTRP15 derived from cardiac myocytes attenuates TGFbeta1-induced fibrotic response in cardiac fibroblasts, *Cardiovasc. Drugs Ther.* 34 (5) (2020) 591–604.
- [25] A. Shokoohi Nahrkhalaji, R. Ahmadi, R. Fadaei, G. Panahi, M. Razzaghi, S. Fallah, Higher serum level of CTRP15 in patients with coronary artery disease is associated with disease severity, body mass index and insulin resistance, *Arch. Physiol. Biochem.* (2019) 1–5.

- [26] R. Ahmadi, R. Fadaei, A. Shokoohi Nahrkhalaji, G. Panahi, S. Fallah, The impacts of C1q/TNF-related protein-15 and adiponectin on Interleukin-6 and tumor necrosis factor-alpha in primary macrophages of patients with coronary artery diseases, *Cytokine* 142 (2021) 155470.
- [27] Y. Zhang, C. Liu, J. Liu, R. Guo, Z. Yan, W. Liu, et al., Implications of C1q/TNF-related protein superfamily in patients with coronary artery disease, *Sci. Rep.* 10 (1) (2020) 878.
- [28] A. Yadav, M.A. Kataria, V. Saini, A. Yadav, Role of leptin and adiponectin in insulin resistance, *Clin. Chim. Acta* 417 (2013) 80–84.
- [29] J. Ramasamy, C. Jagadish, A. Sukumaran, J. Varghese, T. Mani, A.J. Joseph, et al., Low Serum Hepcidin Levels in Patients with Ulcerative Colitis - Implications for Treatment of Co-existent Iron-Deficiency Anemia, 2023. *Inflammation*.
- [30] E. Mina, E. Wyart, R. Sartori, E. Angelino, I. Zaggia, V. Rausch, et al., FK506 bypasses the effect of erythroferrone in cancer cachexia skeletal muscle atrophy, *Cell reports Medicine* (2023) 101306.
- [31] L. Zhang, T. Liu, H. Chen, Q. Zhao, H. Liu, Predicting lncRNA-miRNA interactions based on interactome network and graphlet interaction, *Genomics* 113 (3) (2021) 874–880.
- [32] H.S. Liu, G.F. Ren, H.Y. Chen, Q. Liu, Y.J. Yang, Q. Zhao, Predicting lncRNA-miRNA interactions based on logistic matrix factorization with neighborhood regularized, *Knowl. Base Syst.* (2020) 191.
- [33] L. Zhang, P. Yang, H. Feng, Q. Zhao, H. Liu, Using network distance analysis to predict lncRNA-miRNA interactions, *Interdiscip Sci* 13 (3) (2021) 535–545.
- [34] Y. Yang, N. Huang, L. Hao, W. Kong, A clustering-based approach for efficient identification of microRNA combinatorial biomarkers, *BMC Genom.* 18 (Suppl 2) (2017) 210.
- [35] K.W. Liu, Y. Yang, Incorporating link information in feature selection for identifying tumor biomarkers by using miRNA-mRNA paired expression data, *Curr. Proteomics* 15 (2) (2018) 165–171.
- [36] Y. Yang, Y.Q. Xiao, T.Y. Cao, W. Kong, MiRFFS: a functional group-based feature selection method for the identification of microRNA biomarkers, *Int. J. Data Min. Bioinf.* 18 (1) (2017) 40–55.
- [37] J. Zhang, Z. Zhang, L. Pu, J. Tang, Guo F. Aiepred, An ensemble predictive model of classifier chain to identify anti-inflammatory peptides, *IEEE ACM Trans. Comput. Biol. Bioinf* 18 (5) (2021) 1831–1840.
- [38] H. Wang, Y.J. Ding, J.J. Tang, F. Guo, Identification of membrane protein types via multivariate information fusion with Hilbert-Schmidt Independence Criterion, *Neurocomputing* 383 (2020) 257–269.
- [39] S.I. Abdelsalam, A.M. Alsharif, Y. Abd Elmaboud, A.I. Abdellateef, Assorted kerosene-based nanofluid across a dual-zone vertical annulus with electroosmosis, *Helv. Phys. Acta* 96 (5) (2023).
- [40] M. Iasiello, A. Andreozzi, N. Bianco, K. Vafai, Effects of pulsed radiofrequency source on cardiac ablation, *Bioengineering-Basel.* 10 (2) (2023).
- [41] K. Khanafar, A. Ghosh, K. Vafai, Correlation between MMP and TIMP levels and elastic moduli of ascending thoracic aortic aneurysms, *Cardiovasc. Revascularization Med. : Mol. Interv.* 20 (4) (2019) 324–327.
- [42] M.M. Bhatti, S.M. Sait, R. Ellahi, Magnetic nanoparticles for drug delivery through tapered stenosed artery with blood based non-Newtonian fluid, *Pharmaceuticals* 15 (11) (2022).
- [43] M.M. Bhatti, K. Vafai, S.I. Abdelsalam, The role of nanofluids in renewable energy engineering, *Nanomaterials (Basel, Switzerland)* 13 (19) (2023).
- [44] S.I.I. Abdelsalam, M.M. Bhatti, Unraveling the nature of nano-diamonds and silica in a catheterized tapered artery: highlights into hydrophilic traits, *Sci. Rep.* 13 (1) (2023).